

# Mechanistic Insights on the Stereoselective Nucleophilic 1,2-Addition to Sulfinyl Imines

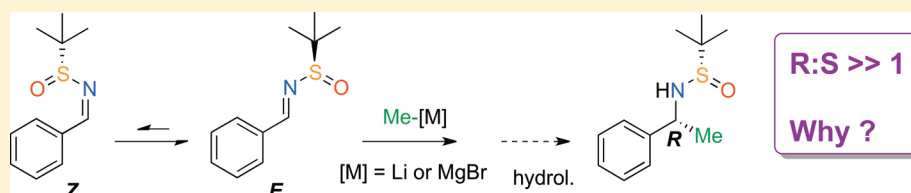
Martin Hennum,<sup>†</sup> Heike Fliegl,<sup>‡</sup> Lise-Lotte Gundersen,<sup>†</sup> and Odile Eisenstein<sup>\*,‡,§</sup>

<sup>†</sup>Department of Chemistry, University of Oslo, P.O. Box 1033, Blindern, N-0315 Oslo, Norway

<sup>‡</sup>Centre for Theoretical and Computational Chemistry, Department of Chemistry, University of Oslo, P.O. Box 1033, Blindern, N-0315 Oslo, Norway

<sup>§</sup>Institut Charles Gerhardt, CNRS 5253, Université Montpellier 2, cc 1501, Place Eugène Bataillon, F-34095 Montpellier, France

**S** Supporting Information



**ABSTRACT:** The asymmetric nucleophilic 1,2-addition of (*S*)-*N*-benzylidene-2-methylpropane-2-sulfinamide with methylmagnesium bromide and methyllithium has been investigated using DFT(B3LYP) computations. The calculated ratio of the two diastereomers agrees with experimental observations, and the factors that determine the diastereomeric ratio are discussed. The preference for the *E* isomer and the rapid equilibrium between the *E* and *Z* isomers of *N*-*tert*-butanesulfinyl imine are two key features for understanding the mechanism of this reaction. Methylmagnesium bromide and methyllithium have bifunctional roles, acting as both Lewis acid and nucleophile, and the Lewis acid character plays a determining role in the stereoselectivity of the reaction.

## INTRODUCTION

Stereoselective addition of organometallics to the C=N bond is a key reaction in the synthesis of pharmaceuticals and natural products.<sup>1</sup> One of the most successful strategies to access highly diverse chiral amines has been the use of *N*-*tert*-butanesulfinyl imines, which have found widespread use as versatile intermediates in asymmetric synthesis. The inherent chirality of sulfinyl imines (–S(O)N=) arises from the pyramidal geometry of sulfur.<sup>2</sup> The lone pair on sulfur has a high barrier of inversion, making sulfinyl imines accessible as nonracemic enantiomers. *N*-*tert*-Butanesulfinyl imines have been used to produce  $\alpha$ -branched and  $\alpha,\alpha$ -dibranched amines,<sup>3</sup> *syn* and *anti* 1,2- or 1,3-amino alcohols,<sup>4</sup> and  $\alpha$ - or  $\beta$ -amino acids and esters,<sup>5</sup> as well as chiral nitrogen containing heterocycles of pyrrolidines, piperidines, and aziridines.<sup>6</sup> Ellman et al. have shown that *N*-benzylidene-2-methylpropane-2-sulfinamide (**1**) reacts easily with Grignard reagents such as methylmagnesium bromide, giving compounds **3** in high diastereomeric excess (97:3) (Scheme 1).<sup>3c</sup> Alkylolithium reagents are also potent nucleophiles but generally yield poorer diastereomeric excesses on reaction with similar sulfinyl imines.<sup>3c</sup>

Sulfinyl imines with two different substituents on the imine carbon exist as *E* and *Z* isomers, which interconvert by inversion of the nitrogen lone pair. The isomerization barrier of *N*-(2-propylidene)arenesulfinamide was found experimentally to be 17 kcal mol<sup>–1</sup>,<sup>7</sup> and that of *N*-ethylidenesulfinamide was calculated to be 24 kcal mol<sup>–1</sup>.<sup>8</sup> As a consequence, *E* and *Z* isomers of sulfinyl imines have not been separated at room

temperature and are in equilibrium. Given this dynamic behavior, the reason for the selectivity of this reaction is not fully understood. Several computational studies have been carried out on asymmetric induction.<sup>9</sup> Targeting the diastereomeric ratio presents two main challenges: evaluating the small difference in energies between the possible intermediates and transition states and including to the best extent the conformational variety of the reactants present. The reaction studied herein is a good illustration of these challenges. In this work, we have used density functional theory (DFT) calculations to study the addition of methylmagnesium bromide and methyllithium to *N*-benzylidene-2-methylpropane-2-sulfinamide (**1**) and determine the diastereomeric ratio (dr) of **2<sub>S</sub>** and **2<sub>R</sub>** (Scheme 1).

## COMPUTATIONAL DETAILS

All calculations were performed with the Gaussian 09 program,<sup>10</sup> using the hybrid functional B3LYP.<sup>11</sup> After a first set of calculations, in which all geometry optimizations were carried out with a 6-31G (d,p) basis set for all atoms,<sup>12</sup> we improved the quality of the study by carrying out the full optimization without any constraint with the cc-pVTZ basis set for all atoms.<sup>13</sup> The reported results are those obtained with the cc-pVTZ basis set, but it is worth noting that they are similar to those obtained with the smaller basis set (similar geometries and relative energies, not differing by more than 5 kcal mol<sup>–1</sup>). Each stationary point was identified as either a minimum or a saddle point

Received: December 17, 2013

Published: March 3, 2014



Scheme 1. Addition of Methyllithium and Methylmagnesium Bromide to (*S*)-*N*-Benzylidene-2-methylpropane-2-sulfonamide, **1**, ([M] = Li, MgBr)

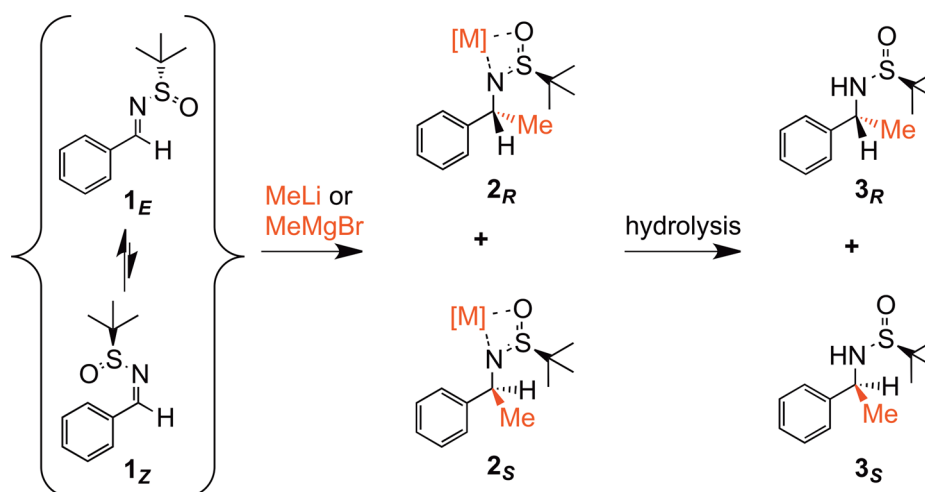


Table 1. Calculated ( $1_E$ ) and Experimental Parameters for the Crystal Structures of Sulfinyl Imines (CCDC Reference Codes)<sup>a</sup>

| molecule             | C–Ar     | C=N      | N–S      | S=O      | S–C      | C–N–S–O |
|----------------------|----------|----------|----------|----------|----------|---------|
| $1_E$ calcd          | 1.465    | 1.276    | 1.727    | 1.498    | 1.898    | 14.0    |
| crystal structures   |          |          |          |          |          |         |
| RAXFOM <sup>20</sup> | 1.465(3) | 1.277(3) | 1.710(2) | 1.484(2) | 1.841(2) | 18.1(2) |
| RAXFUS <sup>20</sup> | 1.466(3) | 1.281(3) | 1.702(2) | 1.487(1) | 1.840(2) | 13.2(2) |
| RAXGAZ <sup>20</sup> | 1.469(3) | 1.275(3) | 1.700(2) | 1.488(2) | 1.846(2) | 17.4(2) |
| COCDA <sup>21</sup>  | 1.457(8) | 1.255(5) | 1.707(5) | 1.470(5) | 1.840(5) | 8.1(4)  |
| VAHYOT <sup>22</sup> | 1.475(4) | 1.279(3) | 1.713(2) | 1.482(2) | 1.851(3) | 13.7(3) |

<sup>a</sup>The distances are in Å, and the CNSO dihedral angles are in deg.

by analytical calculation of the frequencies. The connectivity among reactant, transition state (TS), and product was verified by following the intrinsic reaction coordinates (IRC).<sup>14</sup> The Gibbs energies were calculated within the harmonic approximation of frequencies at  $T = 298.15$  K and  $P = 1$  atm, as well as at 225.15 K, which corresponds to the temperature used in the experimental setting. Values given in the text are those for 225.15 K. Dispersion effects were taken into account by using Grimme's D3 approach, introduced as a single-point correction on the B3LYP/cc-pVTZ optimized geometry.<sup>15</sup> Solvation effects (THF) were included as single-point corrections with the SMD method,<sup>16</sup> as implemented in Gaussian 09. The Gibbs energies were computed by adding the free energy corrections in the gas phase to the energies in solution obtained from the SMD calculations. The energies are also corrected by the dispersion energies calculated in the gas phase. The NBO analysis was carried out using NBO 3.1.<sup>17</sup> Weak noncovalent interactions were visualized on the basis of reduced density gradients using NCIPLOT 2.<sup>18</sup> In this study, we have used the *S* enantiomer of sulfinylimine to provide a direct comparison to the work of Ellman et al.<sup>3c</sup>

## RESULTS

**Structures of *N*-Benzylidene-2-methylpropane-2-sulfonamide (**1**).** The substrate **1** exists as two isomers;  $1_E$ , where the phenyl and sulfoxide groups are *trans* relative to the C=N double bond, and  $1_Z$ , where they are *cis* (Scheme 1). The  $1_E$  isomer is more stable than  $1_Z$  by 10.0 kcal mol<sup>−1</sup>, which is in agreement with the lack of observation of  $1_Z$ .<sup>19</sup> The calculated structure of  $1_E$  compares well with the crystal structures of related systems, which all have an *E* conformation (Table 1).<sup>20–22</sup> In  $1_E$ , the CNSO dihedral angle is 14°, in excellent agreement with the average value of 14° observed in the crystal structures. A search for other conformations varying the CNSO

dihedral angle identified a conformer,  $1_{Eb}$ , 4.4 kcal mol<sup>−1</sup> higher in energy. In the following, we focus on  $1_E$  unless otherwise mentioned. The structural parameters of the Ar–C=N moiety are quantitatively reproduced, but the N–S, S=O and S–C bond lengths are slightly longer than in the experimental structures. The  $1_Z$  isomer has a CNSO dihedral angle of 39° and bond lengths rather similar to those in  $1_E$ , with the exception of the N–S bond, which is longer by 0.03 Å. The  $1_Z$  isomer is disfavored because of the steric repulsion between the phenyl ring and the SO group, resulting in an opening of the C=N–S angle (131.6° in  $1_Z$  vs 112.5° in  $1_E$ ), an out-of-plane twist of the sulfoxide group, and a lengthening of the N–S bond.

The isomerization between  $1_E$  and  $1_Z$  can occur via inversion at the nitrogen or by rotation about the C=N double bond. Test calculations for rotation about the C=N double bond did not yield any transition state, while one was found for nitrogen inversion. The isomerization between the two most stable conformations of  $1_E$  and  $1_Z$  also require a conformational change of the sulfoxide group via rotation about the N–S bond. As a consequence, the isomerization of  $1_E$  to  $1_Z$  first goes through a rotation about the N–S bond with a Gibbs energy barrier of 5.2 kcal mol<sup>−1</sup>, which gives intermediate  $1_{Eb}$ . Then, the isomer  $1_{Eb}$  isomerizes into  $1_Z$  via the transition state  $1_{E-Z}$ -TS (Figure 1) with a Gibbs energy of 19.6 kcal mol<sup>−1</sup> above  $1_E$ , which is within the expected range of values.<sup>7,8</sup> At the transition state for N inversion, the C=N–S angle is 166°. The inversion barrier for the structurally similar compound *N*-ethylidenesulfonamide has been calculated by Bharatam et al. to be 24.2 kcal mol<sup>−1</sup> at the B3LYP/6-31+G\* level of theory.<sup>8</sup> For comparison, the inversion barrier of methyleneimine is

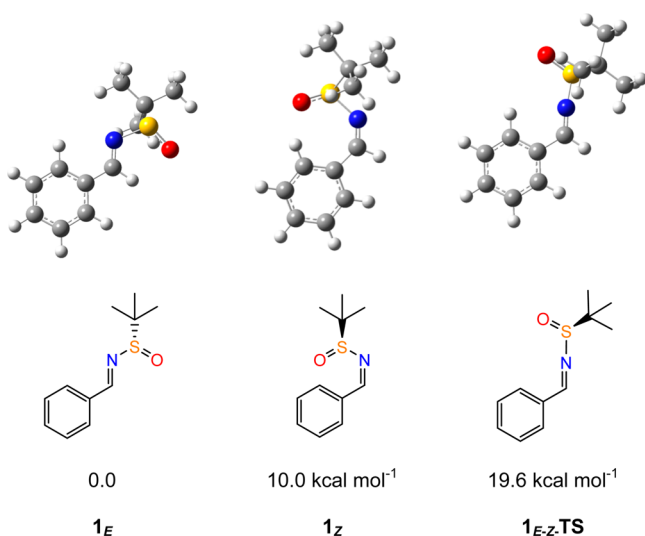


**Figure 1.** *E* and *Z* isomeric structures of **1** and the transition state for isomerization, with energies in kcal mol<sup>−1</sup>. Color scheme: C, gray; N, blue; S, yellow; O, red.

substantially higher (ca. 28–30 kcal mol<sup>−1</sup>).<sup>23</sup> Conjugation is responsible for the lower barrier of isomerization in **1**. As shown in Figure 1, the nitrogen lone pair is always coplanar with the S=O bond and is thus delocalized and stabilized by the  $\sigma^*_{\text{S=O}}$  orbital. NBO analysis confirms that the donation from the N lone pair to the empty  $\sigma^*_{\text{S=O}}$  orbital is present in **1<sub>E</sub>** and **1<sub>Z</sub>** and stronger (about doubled) in the transition state between them, since the lone pair at N is essentially a pure 2p orbital, as the C=N–S angle is widely open.

**Diastereoselectivity of the Addition of MeMgBr and MeLi to 1.** The alkylation reaction has been studied with MeMgBr and MeLi, and we will start by describing the results with MeMgBr (Figure 2). MeLi and MeMgBr were considered as monomeric species in this study. Experimental studies have shown that MeLi, which forms tetramers, reacts as a monomer in THF solution, as established in the case of a reaction with a ketone.<sup>24</sup> Computational studies have used monomeric and dimeric models of MeMgBr and MeLi in related nucleophilic additions, showing that the two models give qualitatively similar results.<sup>25,26</sup>

**(a). Addition of MeMgBr.** MeMgBr forms a stable complex with **1** by coordination to the oxygen. Coordination at nitrogen is found to be less favorable. Coordination to sulfur was ignored, as previous studies have shown that it is not competitive with coordination to N and O.<sup>27</sup> The coordination of MeMgBr to the two isomers of **1** is exoergic, by 14.3 kcal mol<sup>−1</sup> for **1<sub>E</sub>**, forming **1<sub>E-MeMgBr</sub>**, and 18.1 kcal mol<sup>−1</sup> for **1<sub>Z</sub>**, forming **1<sub>Z-MeMgBr</sub>**. In **1<sub>E-MeMgBr</sub>** C, N, S, and O are nearly coplanar (CNSO dihedral angle 19°). In contrast, steric repulsion between the phenyl group and MeMgBr in **1<sub>Z-MeMgBr</sub>** forces the S=O bond out of the plane defined by the phenyl group and the C=N bond (CNSO dihedral angle is 48°). Despite steric repulsions in the latter, **1<sub>Z-MeMgBr</sub>** is only 6.2 kcal mol<sup>−1</sup> above **1<sub>E-MeMgBr</sub>** in energy. The transition state for inversion between these two isomeric complexes is 18.9 kcal mol<sup>−1</sup> above **1<sub>E-MeMgBr</sub>**. Thus, coordination to the Grignard reagent does not influence the kinetic of the isomerization between the *E* and *Z* isomers, and **1<sub>E-MeMgBr</sub>** strongly dominates in the reactive media, in the presence of the Grignard reagent. The Gibbs energy of **1<sub>E-MeMgBr</sub>** is used as the energy reference

in the description of the Gibbs energy profiles. Detailed structural information can be found in the Supporting Information.

The addition of the Grignard reagent can occur from either the *re* or *si* face of the imine, forming a stereogenic center at carbon upon addition of a methyl group. The transition states for the two approaches starting from either **1<sub>E-MeMgBr</sub>** or **1<sub>Z-MeMgBr</sub>** were located. The four transition states **1<sub>E-re-MeMgBr</sub>**-TS, **1<sub>E-si-MeMgBr</sub>**-TS, **1<sub>Z-re-MeMgBr</sub>**-TS, and **1<sub>Z-si-MeMgBr</sub>**-TS are shown in Figure 2. The lowest one (18.0 kcal mol<sup>−1</sup> above reference), **1<sub>E-re-MeMgBr</sub>**-TS, occurs when MeMgBr approaches the *re* side of **1<sub>E-MeMgBr</sub>**. The approach of MeMgBr to the *si* side of the same isomer is 27.0 kcal mol<sup>−1</sup> above the reference. For **1<sub>Z-MeMgBr</sub>**, the approach to the *si* side is preferred over the *re* side, but both transition states are higher in energy than the corresponding transition states in the **1<sub>E-MeMgBr</sub>** isomer. Therefore, there is a strong preference for forming the product originating from **1<sub>E-re-MeMgBr</sub>**-TS. The transition states resulting from **1<sub>Z-MeMgBr</sub>** are higher in energy because the energy barriers associated with the *Z* isomer are higher than those associated with the *E* isomer (23.7 and 27.2 vs 18.0 and 27.0 kcal mol<sup>−1</sup> above **1<sub>Z-MeMgBr</sub>** and **1<sub>E-MeMgBr</sub>**, respectively) and because **1<sub>Z-MeMgBr</sub>** is significantly higher in energy than **1<sub>E-MeMgBr</sub>**. Thus, the dominant product should be **2<sub>R-MgBr</sub>**. The difference in energy between the transition states leading to the *R* and *S* products from **1<sub>E-MeMgBr</sub>** is 11.9 kcal mol<sup>−1</sup>. This difference suggests that **2<sub>S-MgBr</sub>** should not be formed in any detectable quantity. Therefore, the calculations agree with the preference for **2<sub>R</sub>** but overestimate the diastereomeric ratio, since the experimental dr is 97:3.<sup>3c</sup>

After addition of the Grignard reagent, the products are sulfinamides with MgBr coordinated to both O and N (Figure 3). The two products **2<sub>R-MgBr</sub>** and **2<sub>S-MgBr</sub>** are coincidentally at equal energy and exoergic by 18.8 kcal mol<sup>−1</sup>, relative to **1<sub>E-MeMgBr</sub>**.

In all transition states, (Figure 4) the C, N, S, and O atoms from the reactant and the Mg and Me atoms from the Grignard form a six-membered ring with the Mg bonded to O. The distances between the Me carbon and the imine carbon are 2.18 Å (**1<sub>Z-si-MeMgBr</sub>**-TS), 2.29 Å (**1<sub>Z-re-MeMgBr</sub>**-TS), 2.17 Å (**1<sub>E-si-MeMgBr</sub>**-TS), and 2.38 Å (**1<sub>E-re-MeMgBr</sub>**-TS). Counter-intuitively, the preferred TS (**1<sub>E-re-MeMgBr</sub>**-TS) has the longest distance between the nucleophile (Me carbon) and the imine carbon (2.38 Å). The Mg⋯N distances are 3.22 Å (**1<sub>Z-re-MeMgBr</sub>**-TS), 3.18 Å (**1<sub>E-si-MeMgBr</sub>**-TS), 3.17 Å (**1<sub>Z-si-MeMgBr</sub>**-TS), and 2.25 Å (**1<sub>E-re-MeMgBr</sub>**-TS). The decrease in the Mg⋯N distance correlates with the lowering of transition state energies, the shortest distance being associated with the lowest transition state (**1<sub>E-re-MeMgBr</sub>**-TS). Therefore, in the transition state, Mg already interacts with N, to which it will be bonded in the product. The ability of Mg to be close to N in the transition states appears to be an important parameter of the reaction, which has an impact on the diastereoselectivity.

**(b). Reaction of Methylithium with 1.** The study was continued with methylithium, using monomeric MeLi as the representative reagent, and the results are shown in Figure 5. Globally, the results are similar to the reaction with the Grignard reagent (Figure 2). The coordination of MeLi to compound **1** gives a strong preference for **1<sub>E-MeLi</sub>** and the barrier of inversion at the nitrogen is similar to that calculated for **1<sub>E-MeMgBr</sub>** as well as for the uncoordinated **1<sub>E</sub>**.

The energies of the four transition states to form the **2<sub>R</sub>** and **2<sub>S</sub>** isomers from either **1<sub>E-MeLi</sub>** or **1<sub>Z-MeLi</sub>** show that **1<sub>E-re-MeLi</sub>**-TS

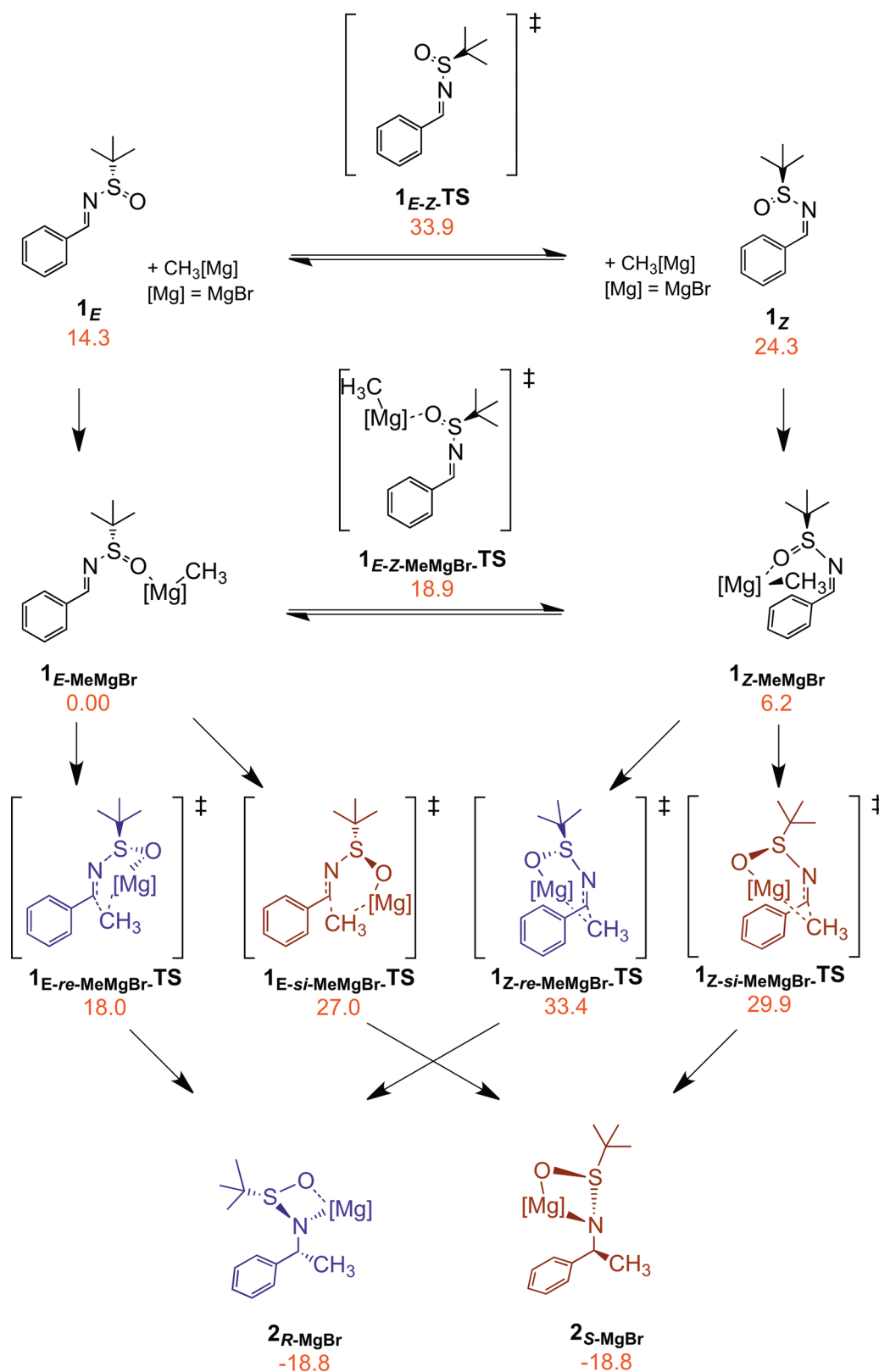


**Figure 2.** Gibbs energy profile (kcal mol<sup>-1</sup>) for the reaction of MeMgBr ([Mg] = MgBr) with 1.

is the lowest in energy and the **1<sub>Z-re-MeLi</sub>-TS** is the highest, while the two other transition states, **1<sub>E-si-MeLi</sub>-TS** and **1<sub>Z-si-MeLi</sub>-TS**, have the same energy (Figure 6). This is only slightly different from the energies obtained with the Grignard reagent, since the preferred transition state (**1<sub>E-re-MeMgBr</sub>-TS**) and the least

preferred transition state (**1<sub>Z-re-MeMgBr</sub>-TS**) are of the same nature.

The transition states form six-membered rings with C (imine), N, S, O, Li, and Me. The lowest energy TS, **1<sub>E-re-MeLi</sub>-TS**, has a rather long C...C distance (2.82 Å) and the shortest



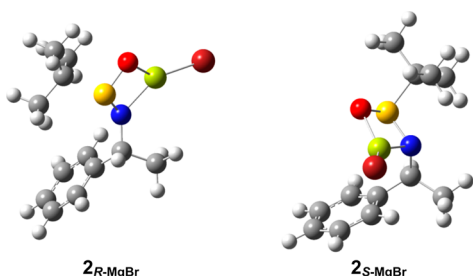


**Figure 3.** Products of the addition of MeMgBr to **1**. Color scheme: C, gray; N, blue; S, yellow; O, red; Mg, lime; Br, burgundy.

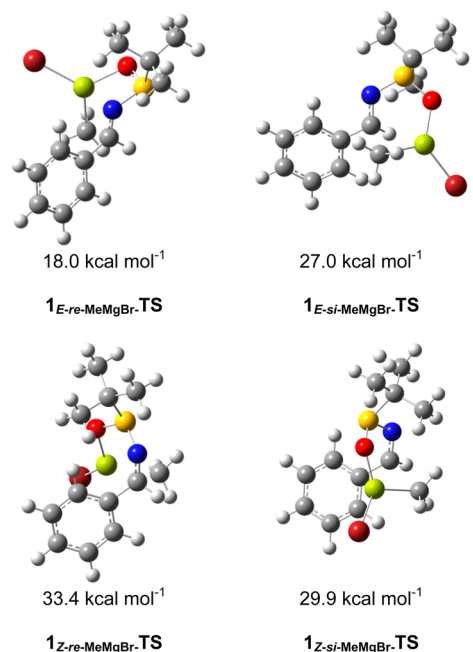


**Figure 4.** Optimized structures of the transition states for the addition of MeMgBr to **1**. The energies given are relative to **1**<sub>E-MeMgBr</sub>. Color scheme: C, gray; N, blue; S, yellow; O, red; Mg, lime; Br, burgundy.

Li...N distance (2.44 Å) among the four transition states. For the Z isomer, the lower energy TS (**1**<sub>Z-si-MeLi</sub>-TS) has an even longer C...C distance (2.99 Å) and a Li...N distance (2.53 Å) shorter than that found in **1**<sub>Z-re-MeLi</sub>-TS.

A consequence of the low barriers for the addition of MeLi to the substrate is that the addition will occur in preference to inversion at nitrogen, whose transition state, via **1**<sub>E-Z-MeLi</sub>-TS, is calculated to be 18.3 kcal mol<sup>-1</sup> above **1**<sub>E-MeLi</sub>. This results in the alkylation occurring almost exclusively via **1**<sub>E-re-MeLi</sub>-TS, which in turn leads to the **2**<sub>R</sub> product. This qualitatively agrees with experimental observations, although in analogy to the reaction with the Grignard reagent, the calculations overestimate the preference for the **2**<sub>R</sub> product. As with Mg, in the **2**<sub>R</sub> product, the Li is coordinated to O and N.

The most significant difference between the reactions with Mg and Li is that the Gibbs energy barriers with MeLi are significantly lower than that with MeMgBr (e.g., **1**<sub>E-re-MeLi</sub>-TS is only 9.3 kcal mol<sup>-1</sup> vs 18.0 kcal mol<sup>-1</sup> with the Grignard reagent, relative to their respective energy references). These low energy barriers agree with the fact that alkyllithiums are usually used at -78 °C, whereas Grignard reagents are used at higher temperatures (often around -48 °C) in reactions with sulfinyl imines.<sup>3b,c</sup>

## DISCUSSION

The four transition states for the nucleophilic addition of a methyl group to the imine carbon of a sulfinyl imine (Figures 2 and 5 for MeMgBr and MeLi, respectively) give two diastereomeric products with an *R* or *S* configuration at carbon adjacent to the nitrogen as the chirality of sulfur is fixed. Each product originates from the approaches to the two faces (*re* or *si*) of the imine, as either the *E* or *Z* isomers. Therefore, the *dr* is controlled by the energy barriers for the nucleophilic addition and by the pre-equilibrium barriers for the isomerization of the *E* and *Z* forms. This pre-equilibrium influences the *dr*, because its associated energy barrier is of the same order of magnitude as the product-forming barriers. Increasing the difference in energy for the approach of the nucleophile to the *re* and *si* sides of the preferred *E* isomer increases the diastereomeric ratio. Increasing the difference in energy between the *Z* and *E* isomers of the sulfinyl imine could achieve the same result. The preferred approach to the less stable *Z* isomer gives the product that is formed by the less preferred route from the *E* isomer. The difference in energy between the *E* and *Z* isomers is controlled, in part, by the interaction, often steric, between the sulfoxide group and the substituents on the imine carbon. If one of the substituents is H and the other is Ph, as in **1**<sub>E</sub>, there is a significant energy preference for the sulfoxide to be in a *cis* relationship to H and in a *trans* relationship to Ph. If the hydrogen of the imine is replaced by a bulkier substituent, the energy difference between the *E* and *Z* isomers should decrease and so also the *dr* in the reaction with MeMgBr or MeLi. This accounts for the experimental observation that an imine derived from an aldehyde (with an H *cis* to the sulfoxide) generally gives a higher *dr* than an imine derived from a ketone (with an R group *cis* to the sulfoxide). The bulky *t*-Bu group on the sulfur atom in compound **1** also affects the diastereoselectivity, as it influences the geometrical features of the six-membered transition states by being forced to occupy a space far from the other atoms. It should be noted that this study was carried out without explicit ethereal solvents coordinated to the metal cation. Although the coordinated solvent could modify the energy profiles of the reaction, the calculated trends obtained in this work qualitatively agree with the experimental data, indicating that the essential factors have been captured by the models and the level of calculation. The quantitative prediction of enantioselectivity is still a challenge for computational methods.<sup>28</sup> In addition, there is room for the solvent to coordinate to the metal outside of the reactive sphere, thereby maintaining the interactions between the MeMgBr or MeLi and the substrate as determined in this study. Furthermore, we have ignored the dissociation of the MeMgBr and MeLi species into their reactive monomeric forms. The qualitative agreement between the calculations and the experimental result that MeLi reacts faster than MeMgBr suggests that the dissociation to the monomers is not the rate-determining step.

The transition states for these additions involve six atoms: the C and N of the imine, the S and O of the sulfoxide, and the organometallic nucleophile. The calculations show that the nucleophile is rather far from the imine carbon and is in fact the farthest away in the lowest respective transition states (**1**<sub>Z-re-MeMgBr</sub>-TS and **1**<sub>Z-re-MeLi</sub>-TS). The metal is bonded to the oxygen at M–O distances between 1.92 and 2.02 Å for Mg and between 1.80 and 1.90 Å for Li. However, the lowest transition state is not associated with the shortest M–O distance. Actually, the metal to nitrogen distance is the shortest

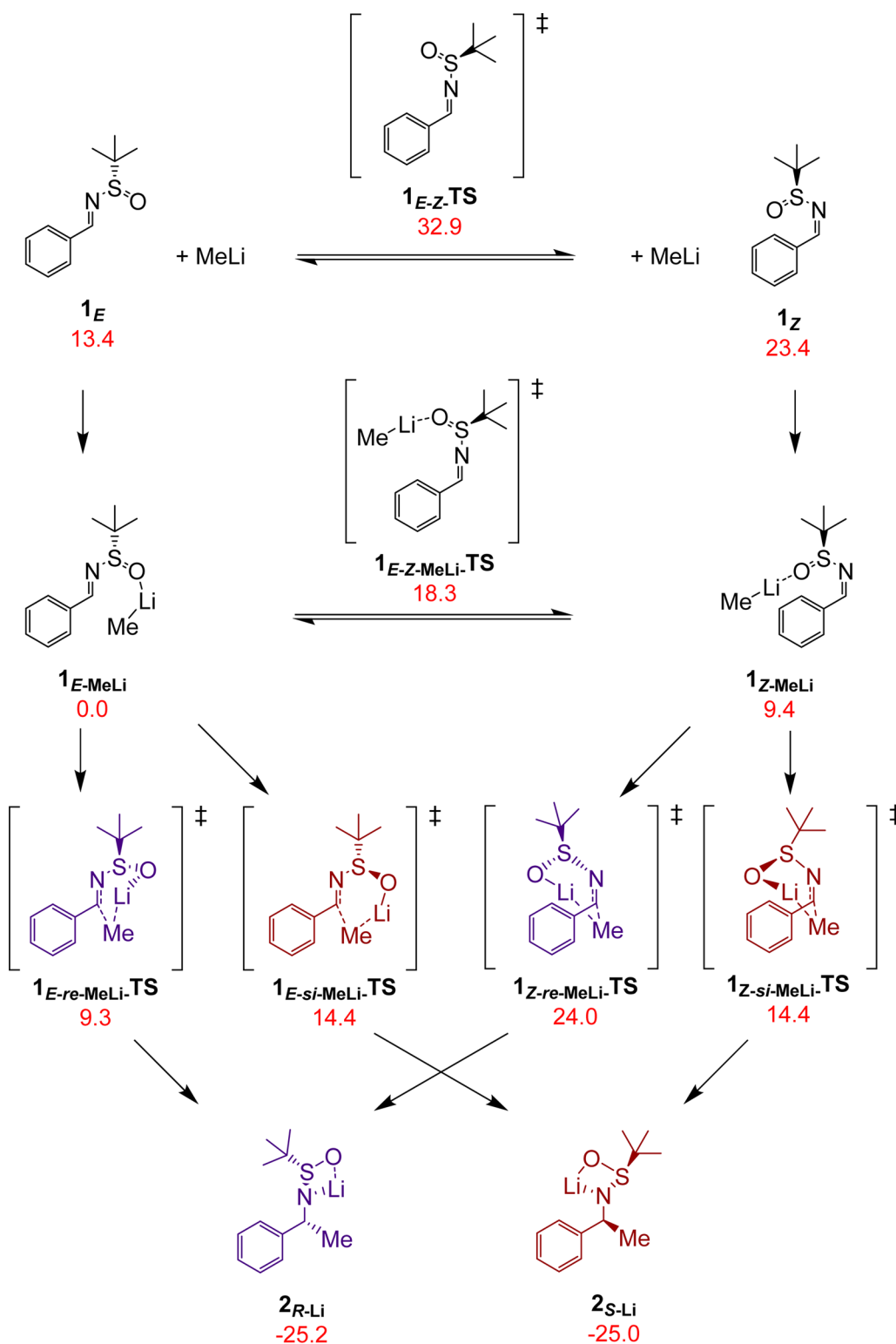


**Figure 5.** Gibbs energy profile (kcal mol<sup>-1</sup>) for the reaction of MeLi with 1.

in the lowest transition state, suggesting that this interaction is important. The natural bond orbital (NBO) analysis reveals though that there is no significant direct delocalization of electron density from the nitrogen to the metal. However, the C=N  $\pi$  bond, which is parallel to the S=O bond, delocalizes into the empty  $\sigma^*_{\text{SO}}$  orbital, whose ability to hyperconjugate is enhanced by the coordination to the Lewis acid. This delocalization is maximal in the lowest transition state. In

order to search for weaker interactions that cannot be traced by the NBO approach, the NCI analysis was used.<sup>18</sup> This analysis reveals the presence of attractive, noncovalent interactions between the methyl group and the imine carbon and also between the metal and the nitrogen, as shown in Figure 7. The corresponding data for all other transition states can be found in the Supporting Information.

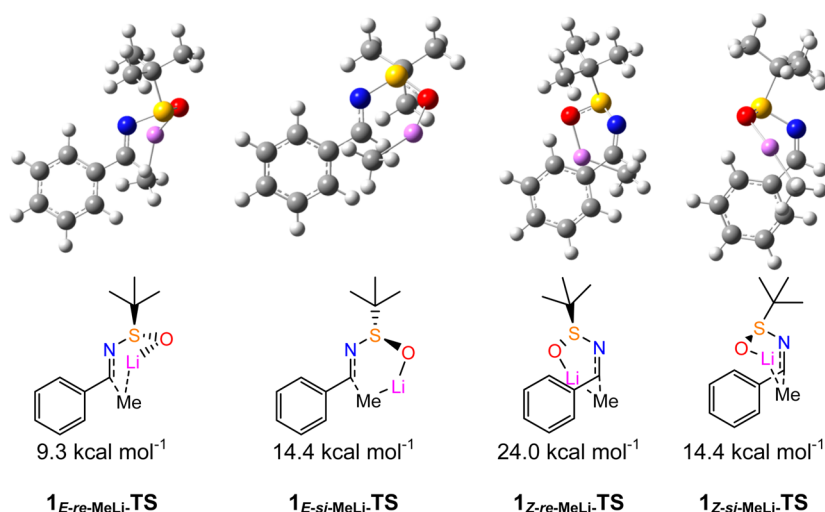


**Figure 6.** Optimized structures of the transition states for the addition of MeLi to 1. Color scheme: C, gray; N, blue; S, yellow; O, red; Li, lilac.

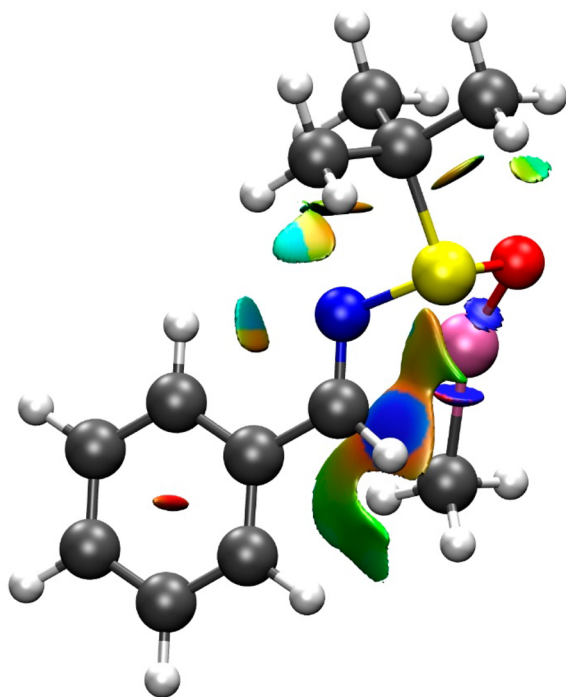


**Figure 7.** NCI plot for 1<sub>E-re</sub>-MeLi-TS showing weak noncovalent interactions (attractive, blue > green; repulsive, yellow < red).

Therefore, even if the methyl group is rather far from the imine carbon, some weak stabilizing interactions are occurring in the transition state. In addition, significant stabilizing interaction is associated with the metal center. Thus, in this nucleophilic addition, a key role is played by the metal, which acts as a Lewis acid. The coordination of the metal to the electron-rich oxygen atom lowers the energy of the  $\sigma^*_{\text{SO}}$  orbital, which enhances the delocalization of the C=N  $\pi$  bond. In turn, this makes the imine carbon more electrophilic. In the optimized geometry of the transition state, there is also a weak M $\cdots$ N interaction. These combined interactions drive the addition of the methyl group to the imine carbon. A previous study of the addition of MeLi to formaldehyde, a reaction in which Li can only coordinate to the oxygen atom, has also demonstrated the role of the Lewis acid in the transition state,

through a shorter Li–O distance in comparison to the carbon methyl distance.<sup>26</sup>

## CONCLUSION

A DFT study of the asymmetric addition of MeMgBr and MeLi to a chiral sulfinyl imine (N-benzylidene-2-methylpropane-2-sulfinamide, 1) reproduces the preference for the major diastereomer. This isomer derives mostly from the preferred approach of the reactant to the more stable *E* isomer of the substrate. However, the *E* to *Z* isomerization, being competitive with the nucleophilic addition, can influence the dr. Thus, increasing the energy gap between the *E* and *Z* isomers increases the dr, and this can be manipulated by having sterically differentiated substituents on the imine carbon. The analyses of the electronic structures of the transition states reveal a key role of the Lewis acid in making the reaction favorable and stereoselective. Particularly, in the lowest transition state, the coordination of the metal to the oxygen makes the imine more electrophilic by delocalization of its  $\pi$  electron density into the  $\sigma^*_{\text{SO}}$  orbital, whose ability to hyperconjugate is increased by the coordination to the metal. Analyses of noncovalent interactions in the transition states reveal that the metal interacts with the nitrogen and the methyl group interacts with the carbon of the imine.

## ASSOCIATED CONTENT

### Supporting Information

Tables and figures giving coordinates of all optimized structures (with graphical representation of the extrema) with *E* and *G* in hartrees, harmonic frequencies, and zero-point energies and additional NCI plots. This material is available free of charge via the Internet at <http://pubs.acs.org>.

## AUTHOR INFORMATION

### Corresponding Author

\*E-mail for O.E.: [odile.eisenstein@univ-montp2.fr](mailto:odile.eisenstein@univ-montp2.fr).

### Notes

The authors declare no competing financial interest.

## ACKNOWLEDGMENTS

M.H. thanks the Research Council of Norway (Grant No. 209330) for funding. H.F. and O.E. acknowledge support by

the Norwegian Research Council through the CoE, Centre for Theoretical and Computational Chemistry (Grant No.179568/V30). O.E. thanks the CTCC for an adjunct professor position and the CNRS and Ministère de l'Enseignement Supérieur et de la Recherche for funding. This work has received support from the Norwegian Supercomputing Program (NOTUR) through a grant of computing time (Grant No. NN4654K).

## REFERENCES

- (1) Bloch, R. *Chem. Rev.* **1998**, 98, 1407.
- (2) Aurisicchio, C.; Baciocchi, E.; Gerini, M. F.; Lanzalunga, O. *Org. Lett.* **2007**, 9, 1939 and references therein.
- (3) (a) Liu, G.; Cogan, D. A.; Ellman, J. A. *J. Am. Chem. Soc.* **1997**, 119, 9913. (b) Cogan, D. A.; Ellman, J. A. *J. Am. Chem. Soc.* **1999**, 121, 268. (c) Cogan, D. A.; Liu, G.; Ellman, J. A. *Tetrahedron* **1999**, 55, 8883.
- (4) (a) Barrow, J. C.; Ngo, P. L.; Pellicore, J. M.; Selnick, H. G.; Nantermet, P. G. *Tetrahedron Lett.* **2001**, 42, 2051. (b) Zhong, Y.-W.; Dong, Y.-Z.; Fang, K.; Izumi, K.; Xu, M.-H.; Lin, G.-Q. *J. Am. Chem. Soc.* **2005**, 127, 11956. (c) Evans, J. W.; Ellman, J. A. *J. Org. Chem.* **2003**, 68, 9948. (d) Kochi, T.; Tang, T. P.; Ellman, J. A. *J. Am. Chem. Soc.* **2003**, 125, 11276. (e) Kochi, T.; Tang, T. P.; Ellman, J. A. *J. Am. Chem. Soc.* **2002**, 124, 6518.
- (5) (a) Avenoza, A.; Busto, J. H.; Corzana, F.; Peregrina, J. M.; Sucunza, D.; Zurbano, M. M. *Synthesis* **2005**, 575. (b) Naskar, D.; Roy, A.; Seibel, W. L.; Portlock, D. E. *Tetrahedron Lett.* **2003**, 44, 8865. (c) Jacobsen, M. F.; Skrydstrup, T. *J. Org. Chem.* **2003**, 68, 7112. (d) Tang, T. P.; Ellman, J. A. *J. Org. Chem.* **2002**, 67, 7819. (e) Tang, T. P.; Ellman, J. A. *J. Org. Chem.* **1999**, 64, 12.
- (6) (a) Morton, D.; Pearson, D.; Field, R. A.; Stockman, R. A. *Synlett* **2003**, 1985. (b) Denolf, B.; Manginckx, S.; Törnroos, K. W.; Kimpe, N. D. *Org. Lett.* **2006**, 8, 3129. (c) Chemla, F.; Ferreira, F. J. *Org. Chem.* **2004**, 69, 8244. (d) Schenkel, L. B.; Ellman, J. A. *Org. Lett.* **2004**, 6, 3621. (e) Brinner, K. M.; Ellman, J. A. *Org. Biomol. Chem.* **2005**, 3, 2109.
- (7) (a) Davis, F. A.; Friedman, A. J.; Kluger, E. W. *J. Am. Chem. Soc.* **1974**, 96, 5000. (b) Davis, F. A.; Friedman, A. J.; Nadir, U. K. *J. Am. Chem. Soc.* **1978**, 100, 2844. (c) Davis, F. A.; Reddy, R. E.; Szweczyk, J. M.; Reddy, G. V.; Portonovo, P. S.; Zhang, H.; Fanelli, D.; Reddy, R. T.; Zhou, P.; Carroll, P. J. *J. Org. Chem.* **1997**, 62, 2555.
- (8) Bharatam, P. V.; Uppal, P.; Kaur, A.; Kaur, D. *J. Chem. Soc., Perkin Trans. 2* **2000**, 43.
- (9) (a) Allemann, C.; Gordillo, R.; Clemente, F. R.; Cheong, P.-Y.; Houk, K. N. *Acc. Chem. Res.* **2004**, 37, 558. (b) Houk, K. N. *Theor. Chem. Acc.* **2000**, 103, 330. (c) Balcells, D.; Maseras, F. *New J. Chem.* **2007**, 31, 333. (d) Mengel, A.; Reiser, O. *Chem. Rev.* **1999**, 99, 1191. (e) Anh, N. T.; Eisenstein, O. *Nouv. J. Chim.* **1977**, 1, 61.
- (10) Frisch, M. J.; Trucks, G. W.; Schlegel, H. B.; Scuseria, G. E.; Robb, M. A.; Cheeseman, J. R.; Scalmani, G.; Barone, V.; Mennucci, B.; Petersson, G. A.; Nakatsuji, H.; Caricato, M.; Li, X.; Hratchian, H. P.; Izmaylov, A. F.; Bloino, J.; Zheng, G.; Sonnenberg, J. L.; Hada, M.; Ehara, M.; Toyota, K.; Fukuda, R.; Hasegawa, J.; Ishida, M.; Nakajima, T.; Honda, Y.; Kitao, O.; Nakai, H.; Vreven, T.; Montgomery, J. A., Jr.; Peralta, J. E.; Ogliaro, F.; Bearpark, M.; Heyd, J. J.; Brothers, E.; Kudin, K. N.; Staroverov, V. N.; Kobayashi, R.; Normand, J.; Raghavachari, K.; Rendell, A.; Burant, J. C.; Iyengar, S. S.; Tomasi, J.; Cossi, M.; Rega, N.; Millam, N. J.; Klene, M.; Knox, J. E.; Cross, J. B.; Bakken, V.; Adamo, C.; Jaramillo, J.; Gomperts, R.; Stratmann, R. E.; Yazyev, O.; Austin, A. J.; Cammi, R.; Pomelli, C.; Ochterski, J. W.; Martin, R. L.; Morokuma, K.; Zakrzewski, V. G.; Voth, G. A.; Salvador, P.; Dannenberg, J. J.; Dapprich, S.; Daniels, A. D.; Farkas, Ö.; Foresman, J. B.; Ortiz, J. V.; Cioslowski, J.; Fox, D. J. *Gaussian 09, Revision D.01*; Gaussian, Inc., Wallingford, CT, 2009.
- (11) (a) Becke, A. D. *J. Chem. Phys.* **1993**, 98, 5648. (b) Lee, C.; Yang, W.; Parr, G. *Phys. Rev. B* **1988**, 37, 785. (c) Vosko, S. H.; Wilk, L.; Nusair, M. *Can. J. Phys.* **1980**, 58, 1200. (d) Stephens, P. J.; Devlin, F. J.; Chabalowski, C. F.; Frisch, M. J. *J. Phys. Chem.* **1994**, 98, 11623.
- (12) (a) Petersson, G. A.; Bennett, A.; Tensfeldt, T. G.; Al-Laham, M. A.; Shirley, W. A.; Mantzaris, J. *J. Chem. Phys.* **1988**, 89, 2193. (b) Petersson, G. A.; Al-Laham, M. A. *J. Chem. Phys.* **1991**, 94, 6081.
- (13) (a) Dunning, J. T. H. *J. Chem. Phys.* **1989**, 90, 1007. (b) Kendall, R. A.; Dunning, J. T. H.; Harrison, R. J. *J. Chem. Phys.* **1992**, 96, 6796. (c) Woon, D. E.; Dunning, J. T. H. *J. Chem. Phys.* **1993**, 98, 1358. (d) Peterson, K. A.; Woon, D. E.; Dunning, J. T. H. *J. Chem. Phys.* **1994**, 100, 7410. (e) Wilson, A. K.; van Mourik, T.; Dunning, J. T. H. *J. Mol. Struct. (THEOCHEM)* **1996**, 388, 339.
- (14) (a) Fukui, K. *Acc. Chem. Res.* **1981**, 14, 363. (b) Hratchian, H. P.; Schlegel, H. B. In *Theory and Applications of Computational Chemistry*; Elsevier: Amsterdam, 2005; pp 195–249.
- (15) Grimme, S.; Antony, J.; Ehlrich, S.; Krieg, H. *J. Chem. Phys.* **2010**, 132, 154104.
- (16) Marenich, A. V.; Cramer, C. J.; Truhlar, D. G. *J. Phys. Chem. B* **2009**, 113, 6378.
- (17) Glendenning, E. D.; Reed, A. E.; Carpenter, J. E.; Weinhold, F. *NBO Version 3.1*; University of Wisconsin, Madison, WI.
- (18) (a) Johnson, E. R.; Keinan, S.; Mori-Sánchez, P.; Contreras-García, J.; Cohen, A. J.; Yang, W. *J. Am. Chem. Soc.* **2010**, 132, 6498. (b) Contreras-García, J.; Johnson, E. R.; Keinan, S.; Chaudret, R.; Piquemal, J.-P.; Beratan, D. N.; Yang, W. *J. Chem. Theory Comput.* **2011**, 7, 625.
- (19) Liu, G.; Cogan, D. A.; Owens, T. D.; Tang, T. P.; Ellman, J. A. *J. Org. Chem.* **1999**, 64, 1278.
- (20) Jiang, W.; Marinkovic, D.; Tran, J. A.; Chen, C. W.; Arellano, L. M.; White, N. S.; Tucci, F. C. *J. Org. Chem.* **2005**, 70, 8924.
- (21) Zhu, C.; Shi, Y.; Xu, M.-H.; Lin, G.-Q. *Org. Lett.* **2008**, 10, 1243.
- (22) Owens, T. D.; Souers, A. J.; Ellman, J. A. *J. Org. Chem.* **2003**, 68, 3.
- (23) Lehn, J.-M. *Chem. Eur. J.* **2006**, 12, 5910 and references cited therein.
- (24) (a) Reich, H. J. *Chem. Rev.* **2013**, 113, 7130. (b) Smith, S. G.; Charbonneau, L. F.; Novak, D. P.; Brown, T. L. *J. Am. Chem. Soc.* **1972**, 94, 7059.
- (25) (a) Merino, P.; Franco, S.; Gascon, J. M.; Merchan, F. L.; Tejero, T. *Tetrahedron: Asymmetry* **1999**, 10, 1867. (b) Fressigné, C.; Maddaluno, J.; Marquez, A.; Giessner-Pretre, C. *J. Org. Chem.* **2000**, 65, 8899. (c) Merino, P.; Tejero, T. *Tetrahedron* **2001**, 57, 8125. (d) Mori, T.; Kato, S. *J. Phys. Chem. A* **2009**, 113, 6158.
- (26) Kaufmann, E.; Schleyer, P. v. R.; Houk, K. N.; Wu, Y. D. *J. Am. Chem. Soc.* **1985**, 107, 5560.
- (27) Dobrowolski, J. C.; Kawęcki, R. *J. Mol. Struct. (THEOCHEM)* **2005**, 734, 235.
- (28) Brown, J. M.; Deeth, R. J. *Angew. Chem., Int. Ed.* **2009**, 48, 4476.

## NOTE ADDED AFTER ASAP PUBLICATION

This paper was published ASAP on March 11, 2014. The Abstract graphic was updated. The revised paper was reposted on March 13, 2014.